Modelling ion channel dynamics through reflected stochastic differential equations

Ciara E. Dangerfield,[1,*] David Kay,[1,†] and Kevin Burrage[1,2,‡]

[1] *Department of Computer Science, University of Oxford, Wolfson Building, Parks Road, Oxford, OX1 3QD, UK*

[2] *Department of Mathematics, Queensland University of Technology, Brisbane, Queensland, Australia*

(Dated: April 27, 2012)

Ion channels are membrane proteins that open and close at random and play a vital role in the electrical dynamics of excitable cells. The stochastic nature of the conformational changes these proteins undergo can be significant, however current stochastic modelling methodologies limit the ability to study such systems. Discrete-state Markov chain models are seen as the 'gold-standard', but are computationally intensive, restricting investigation of stochastic effects to the single cell level. Continuous stochastic methods that use stochastic differential equations (SDEs) to model the system are more efficient but can lead to simulations that have no biological meaning. In this paper we show that modelling the behaviour of ion channel dynamics by a reflected SDE ensures biologically realistic simulations and we argue that this model follows from the continuous approximation of the discrete-state Markov chain model. Open channel and action potential statistics from simulations of ion channel dynamics using the reflected SDE are compared with those of a discrete-state Markov chain method. Results show that the reflected SDE simulations are in good agreement with the discrete-state approach. The reflected SDE model therefore provides a computationally efficient method to simulate ion channel dynamics, whilst preserving the distributional properties of the discrete-state Markov chain model and also ensuring biologically realistic solutions. This framework could easily be extended to other biochemical reaction networks.

PACS numbers: 87.10.Mn, 87.19.ll, 87.19.lc, 87.19.Hh
Keywords: Hodgkin-Huxley model; Reflected stochastic differential equations; Ion channels; Membrane noise

I. INTRODUCTION

Ion channels are multiconformational proteins that form a pore in the membrane of excitable cells. They open and close due to conformational changes in the protein as a result of variations in membrane potential, and thus regulate the movement of ions across the lipid bilayer (see for example the review [1]). The dynamics of these proteins are therefore one of the fundamental elements in the generation of an action potential (AP) in excitable cells, [2].

Single-channel recordings demonstrated that the conformational changes the protein undergoes as it opens and closes occur at random, [3]. This internal stochasticity causes fluctuations in individual ionic conductances, [2], and has been shown to have important effects on the electrical dynamics of the whole cell, [4], [5], [6], [7]. In neuronal cells, for example, stochastic ion channel behaviour can modify a number of electrical properties of the cell including the firing threshold [8] and spike timings [9]. Furthermore, in cardiac myocytes this intrinsic randomness leads to variability in the duration of successive APs, [5], [6], termed beat-to-beat variability, which is thought to be an indicator of potential life-threatening arrhythmias, [10]. It can even cause alterations to the AP morphology under pathological conditions, resulting in the formation of early after depolarisations (EADs), [5].

Cells are not isolated entities, but are self-organised in complex multiscale systems such as the heart and neural networks. Therefore, successful physiological investigation requires an understanding not just of isolated cell dynamics, but also the way in which these cells interact at the tissue and whole organ level [11]. For example, in [5] the authors demonstrate that the coupling together of cardiac myocytes via gap junctions, greatly reduces the variability in AP duration and can stop the formation of EADs, both phenomena observed at the single-cell level. Therefore the stochastic effects at single-cell level do not directly translate to the tissue level. The issue is that current stochastic simulation techniques have restricted the investigation into the effects of channel noise at the tissue level, since these methods are typically very computationally intensive.

* ciara.dangerfield@dtc.ox.ac.uk
† dkay@cs.ox.ac.uk
‡ kevin.burrage@cs.ox.ac.uk

Traditionally an ion channel is considered to transition between a discrete set of states at rates that depend upon the membrane potential [2]. The probability of the channel residing in a particular state in the future is assumed to depend only on the current state of the channel, [2]. For a collection of N channels, the evolution in the number of channels in each state can therefore be modelled as a discrete-state continuous-time Markov chain [12]. The change over time in the probability distribution of this process is described by a partial differential equation (PDE) called the Master equation [13], [14], or more commonly referred to as the forward Kolmogorov equation in the probability literature [15]. In the case of the classical Hodgkin-Huxley model, [16], Austin [17] shows that in the limit $N \to \infty$ the Master equation converges to the standard deterministic equations. Indeed this has also been shown for more general systems of chemical reaction networks, (see for example [14], [18]). The Master equation can be solved directly [19], [20], or individual realisations of the process can be simulated exactly using the Gillespie-type algorithm [21], also referred to as the Stochastic Simulation Algorithm (SSA) [22]. While such a discrete-state modelling and simulation approach is often seen as the 'gold-standard', it becomes increasingly computationally costly as the number of channels increases above a few hundred, [23]. Furthermore, since the system is random, each simulation will produce a different realisation and so many simulations are needed in order to make inferences about the general behaviour of the system. Thus, incorporating such an approach into a multiscale modelling environment can become computationally intractable.

In recent years this has led to the increasing popularity of using stochastic differential equations (SDEs) to describe ion channel behaviour [24], [5], [25]. Fox and Lu [26] were the first to take such an approach which they applied to the Hodgkin-Huxley model, and their method has since been extensively used to model neuronal cells [24], [25], cardiac myocytes [5], [6] and pancreatic beta cells [7]. Their approach reduces the dynamics of the whole channel to the collective behaviour of a series of gating variables that can be either open or closed. The proportion of each gating variable in the open state is described by an SDE and the proportion of open channels is given by the product of the open gates. Essentially, Fox and Lu [26] extend the deterministic Hodgkin-Huxley model directly by incorporating a noise term into the equations that describe the gating variables so that they become SDEs. This method leads to orders of magnitude speed up in the computational time of each simulation over the traditional discrete-state Markov chain model [23]. However, a number of studies have demonstrated discrepancies between the SDE and discrete-state Markov chain model, questioning as to whether an SDE model could accurately capture the stochastic dynamics of the discrete-state Markov chain [23], [27], [28].

A recent study by Goldwyn et al. [29] showed that the discrepancies between the two approaches occurs due to the formulation of the SDE model. The authors demonstrate that constructing the SDE model in terms of the kinetic behaviour of the channel, rather than the individual gating variables, preserves the stochastic behaviour of the discrete-state Markov chain model. They refer to the SDE they implement, originally derived in [26], as a channel-based SDE and that of the Fox and Lu approach a subunit-based SDE. Throughout this paper we shall adopt the channel-based approach to formulate the SDE model of ion channel dynamics, given in [29], and so for simplicity shall refer to this as the SDE model, rather than the channel-based SDE. The work of Goldwyn et al. emphasised that the structure of the ion channel dynamics is critical for formulating the SDE model, see the recent review [30] for a further discussion.

However, issues remain with this approach which question the physical meaning of such a model. The solutions of the SDE model provide the evolution in the proportion of channels in each state. Therefore the solution to the SDE must remain non-negative for the path to have any biological relevance. Yet it has been shown that the solution can become negative [31]. Furthermore, since the noise term in the SDE model involves the square root of some function of the state variable, this can result in numerical solutions becoming imaginary [31]. Alterations to the numerical scheme can be made to force the solution to remain positive, for example the Wiener increment can be continually resampled [5]. However such alterations can bias the results [31], [32], [33]. Another approach is to replace the variable (i.e. the state of the system) in the noise term with its equilibrium value, [29], [24] so that the square root term is independent of the state of the system. However, such an approach can still result in the proportion of channels becoming negative, [29].

In [31] a hybrid simulation method for the Hodgkin-Huxley model was developed that attempts to improve the computational efficiency of the discrete-state Markov chain model whilst ensuring individual simulations remain non-negative. The hybrid method switches to the discrete-state Markov

chain model when the chance of negative solutions to the SDE model is high. Such an approach has been shown to increase computational efficiency as well as reduce the chance of biologically unrealistic simulations of ion channel dynamics. However, the optimal time to switch from one regime to another is unclear, and the computational speed ups are not sufficient to incorporate this method into a multiscale environment, [31].

In this paper we address the issue of ensuring biologically realistic solutions to the SDE model, without potentially biasing the solution, by describing a technique for incorporating boundaries into the SDE. The resulting model is commonly termed a reflected SDE and has previously been used to model constrained animal motion [34], human metabolic processes [35] and in a stochastic hybrid model of biochemical reaction kinetics [36]. However, to the best of our knowledge this is the first time that ion channel dynamics have been described using such a formulation. We argue that the reflected SDE is the correct equation that describes the individual realisations of the diffusion process, obtained from the system size expansion of the discrete-state Markov chain model. Using reflected SDEs to model the sodium and potassium channels in the Hodgkin-Huxley model, we show through simulation that the behaviour of the reflected SDE is consistent with the discrete-state Markov chain model. Furthermore, we show that the approximation to the SDE made by Goldwyn et al. [29] is not always valid and in such cases the reflected SDE is in better agreement with the dynamics of the discrete-state Markov chain model. We conclude that the reflected SDE provides a computationally efficient model of ion channel dynamics that faithfully preserves the stochastic dynamics of the discrete-state Markov chain model, whilst also ensuring biologically meaningful simulations.

In the next section, we discuss the mathematical theory of the discrete-state Markov chain model and the approximation of the dynamics by the SDE, for a simple ion channel model. This section contains no new material but rather provides the mathematical background that underpins one of the key outcomes of this paper, namely that the reflected SDE model is the appropriate equation to describe the approximation from the discrete-state Markov chain model, while the SDE without reflection is not. In Secs. III and IV we describe the main novel concepts of this work, demonstrating that using a reflected SDE to describe the dynamics of the approximate continuous process is the correct way in which to incorporate boundary conditions into the SDE model to ensure biologically realistic solutions. We first introduce the reflected SDE using the simple ion channel model given in Sec. III. We then extend these methods to general models of ion channel dynamics and in Sec V we discuss the numerical method used in this paper to approximate solutions to the reflected SDE. The Hodgkin-Huxley model, [16], is used to test the accuracy of the reflected SDE method against the 'gold-standard' Markov chain model. The reflected SDEs for the sodium and potassium channels in the Hodgkin-Huxley model are formulated in Sec. VI. Sec. VII describes the different simulation protocols undertaken to compare the reflected SDE and discrete-state Markov chain models and in Sec. VIII we briefly describe the results of the simulations.

Finally in Sec. IX we outline the key contributions of this paper in the context of the previous work on SDE models of ion channel dynamics. In particular we discuss how the methodology outlined here may be applicable to a wider set of biologically modelling problems than ion channel dynamics alone. We also review the combined impact of this paper and the work of Goldwyn et al. [29] in the fields of neuroscience and cardiac modelling.

II. SIMPLE MODEL OF ION CHANNEL DYNAMICS

Throughout this section random variables are denoted by capital letters and individual realisations of these variables by lower case letters. Bold type is used to denote vectors while scalar values are given in standard type.

The simplest model of an ion channel is to assume that it can be in one of two states, open, O, or closed, C, at time t.

$$C \underset{b}{\overset{a}{\rightleftharpoons}} O$$

For a collection of N ion channels let the entries of the vector $\boldsymbol{X}(t) = (X_1(t), X_2(t))^T$ denote the number of channels in the open and closed states, respectively. If the system is currently in state $\boldsymbol{x}(t)$, then the probabilities of transitioning from closed to open, or open to closed in a small time interval $[t, t + \Delta_t)$ are respectively $ax_2\Delta_t$ and $bx_1\Delta_t$. The transition rates, a and b, are usually assumed to depend on the membrane potential V, which for small Δ_t can be assumed to remain constant over the time step. Therefore, from here on we shall consider the transition rates a and b to be constant over a small time step of size Δ_t.

A. Discrete-state stochastic model

The process $\boldsymbol{X}(t)$ is conventionally modelled as a discrete-state continuous-time Markov chain and the total number of channels N is assumed to remain constant, [12]. Therefore $\boldsymbol{X}(t)$ will take values on the two dimensional integer lattice $[0,\, N]\times[0,\, N]$. Since N is constant, $X_2 = N - X_1$ and so only the number of channels in the open state, which we denote by $X(t)$, need to be considered.

Let $P\,(x,\, t)$ be the probability that the system is in state x (which is integer-valued) at time t, given some initial state x_0. The evolution of the system can be described by a PDE called the Master equation [13], [14] or the forward Kolmogorov equation [15],

$$\begin{aligned}\frac{\partial P(x,t)}{\partial t} &= a(N-(x-1))P(x-1,t) \\ &\quad + b(x+1)P(x+1,t) \\ &\quad - (bx + a(N-x))P(x,t) \\ &\quad \text{for } 0 < x < N \qquad x \in \mathbb{N}.\end{aligned} \tag{1}$$

Since the total number of channels remains constant, the following condition must be satisfied

$$\sum_{x=0}^{N} \tfrac{\partial P(x,t)}{\partial t} = 0.$$

Using this, along with the fact that $X(t)$ cannot be negative or greater than N, $P(x,t)$ must satisfy the following equations at the boundary of the interval $[0, N]$.

$$\begin{aligned}\frac{\partial P(0,t)}{\partial t} &= bP(1,t) - aNP(0,t), \\ \frac{\partial P(N,t)}{\partial t} &= aP(N-1,t) - bNP(N,t).\end{aligned}$$

As the number of channels increases, simulating the dynamics of this discrete-state Markov chain becomes increasingly computationally intensive, restricting the incorporation of such methods into multiscale models. This has lead to the development of models that approximate the dynamics of this system.

B. Background: Approximating ion channel dynamics by a diffusion model

In this section we discuss the approximation of the discrete-state Markov chain by a continuous-state model using the system size expansion approach of Van Kampen [14]. For the Hodgkin-Huxley model [16] much of the mathematical theory underlying this limit was presented by Pakdaman et al. [37] and Fox and Lu [26]. In these works, the authors explicitly take into account the voltage dependence of the transition rates. Since we assume that the transition rates are constant on a given time step, we give a simpler presentation of the mathematical theory largely based on [14].

As the number of channels becomes large, it makes sense to think of the state of the system in terms of proportions of channels in a certain state rather than discrete numbers. Therefore we consider the behaviour of the scaled process $Y(t) = X(t)/N$. For ease of notation we let $\tilde{y} = y - \frac{1}{N}$ and $\hat{y} = y + \frac{1}{N}$. The master equation, (1), thus becomes

$$\begin{aligned}\frac{\partial P(y,t)}{\partial t} &= N\left[a(1-\tilde{y})P(\tilde{y},t) + b\hat{y}P(\hat{y},t)\right] \\ &\quad - N\left[by + a(1-y)\right]P(y,t) \\ &\quad \text{for } 0 < y < 1 \qquad y \in \mathbb{R}.\end{aligned} \tag{2}$$

Note we have not considered the behaviour of the system at the boundary. We shall deal with the boundary conditions for this system in the next section.

Consider taking the Taylor expansion of the first two terms in (2) about the point y. We assume that N is large enough so that terms of order greater than two can be considered negligible [14], [26]. The first two terms can thus be approximated by the following expressions,

$$\begin{aligned}&a(1-\tilde{y})P(\tilde{y},t) \approx a(1-y)P(y,t) \\ &- \tfrac{1}{N}\tfrac{\partial}{\partial y}\left(a(1-y)P(y,t)\right) + \tfrac{1}{2N^2}\tfrac{\partial^2}{\partial y^2}\left(a(1-y)P(y,t)\right),\end{aligned} \tag{3}$$

$$\begin{aligned}&b(\hat{y})P(\hat{y},t) \approx byP(y,t) + \tfrac{1}{N}\frac{\partial}{\partial y}\left(byP(y,t)\right) \\ &+ \tfrac{1}{2N^2}\frac{\partial^2}{\partial y^2}\left(byP(y,t)\right).\end{aligned} \tag{4}$$

Replacing these terms in (2) by the appropriate expansion we obtain a PDE called the Fokker-Planck equation, [14], [26],

$$\begin{aligned}\frac{\partial P(y,t)}{\partial t} &= -\tfrac{\partial}{\partial y}\left[(a-\alpha y)\,P(y,t)\right] \\ &\quad + \tfrac{1}{2N}\tfrac{\partial^2}{\partial y^2}\left[(a+\beta y)\,P(y,t)\right],\end{aligned} \tag{5}$$

where $\alpha = a + b$, $\beta = b - a$.

This equation describes the evolution in the probability distribution of a continuous-state continuous-time Markov chain model, which is frequently referred to as a diffusion process [15]. In moving from (1) to (5) we effectively assume that for large enough N, the dynamics of the discrete-state Markov chain can be well approximated by those of the diffusion process.

It is well known that the sample paths of a diffusion process can be described by an SDE [38] and in the case of (5) this takes the form of the following Langevin equation, [39], [40]

$$dY = (a - \alpha Y)\, dt + \tfrac{1}{\sqrt{N}}\sqrt{a + \beta Y}\, dW, \qquad (6)$$

where, $W(t)$ is a Wiener process whose increments $dW = W(t + \Delta_t) - W(t)$ are independent and normally distributed with mean 0 and variance Δ_t.

The advantage of describing ion channel dynamics in this way is that a single path of an SDE can be simulated with comparable efficiency to that of an ordinary differential equation (ODE), and so greatly improves the computational efficiency of the discrete-state Markov chain model. The simplest method for numerically solving an SDE is the Euler-Maruyama method, see [41] for example. In the case of (6) this leads to

$$\begin{aligned} y(t + \Delta_t) = y(t) + (a - \alpha y(t))\, \Delta_t \qquad (7) \\ + \tfrac{1}{\sqrt{N}}\sqrt{a + \beta y(t)}\Delta W_t, \end{aligned}$$

where Δ_t is the time interval and ΔW_t is a Wiener increment. However, there are issues with ensuring biologically realistic solutions to (6).

Making the transformation $U(t) = a + \beta Y(t)$, based on (6) and using Itô's formula, [41], the transformed process can be described by the following SDE,

$$dU = (2ab - \alpha U)dt + \tfrac{\beta}{\sqrt{N}}\sqrt{U}dW.$$

This equation is commonly known as the Cox, Ingersoll and Ross (CIR) model [42] and was first proposed by Feller to model population dynamics [43]. In particular, Feller showed that there exists a non-negative solution to (8). Transforming back to the original process $Y(t)$, this suggest that $Y(t) \geq \frac{-a}{\beta}$ if $a < b$ or otherwise $Y(t) \leq \frac{-a}{\beta}$. Therefore the process $Y(t)$ can become negative or greater than one and for such values $Y(t)$ has no physical meaning, [31].

In spite of this, (6) is a popular model used to simulate ion channel dynamics, where authors often implement alterations to the numerical scheme (for example in (7)) in order to force the discrete approximations to remain within the desired region [5], [24]. However, the real issue stems from the form of (6) rather than the numerical approximation.

The SDE gives the individual realisations of the diffusion process $Y(t)$ whose probability distribution is governed by the Fokker-Planck equation (5). While we can impose boundary conditions onto the Fokker-Planck equation to ensure the probability of $Y(t)$ taking values outside $[0, 1]$ is 0, in switching to the SDE formulation of the problem these boundary conditions have in some sense become 'lost'. In the next section we show how these boundary conditions can be incorporated into the SDE, thus providing a formulation for the sample paths of the diffusion process that is consistent with the dynamics of the Fokker-Planck equation.

III. REFLECTED STOCHASTIC DIFFERENTIAL EQUATIONS

Returning to the construction of the Fokker-Planck equation, (5), we require that the diffusion process, $Y(t)$, must remain in $[0, 1]$ for all time. Using this, along with the fact that the probability density function $P(y, t)$ must integrate to 1, the following relation must hold

$$\int_0^1 P(y, t)dy = 1,$$

and so

$$\frac{\partial}{\partial t}\int_0^1 P(y, t)dy = 0.$$

Interchanging the integral and the derivative with respect to t in the above formula and using the relation (5) it follows that

$$(a - \alpha y)\, P(y, t) - \tfrac{1}{2N}\tfrac{\partial}{\partial y}\left[(a + \beta y)\, P(y, t)\right] = 0, \quad (8)$$

at the boundaries $y = 0$ and $y = 1$, [14].

Since the condition (8) reflects the solution back into the interval $(0, 1)$ at the boundaries, the process $Y(t)$ is often referred to as a reflected diffusion.

In the previous section we noted that the approximation of (1) by (5) only holds for large N, and so for small N the diffusion process may no longer accurately capture the dynamics of the discrete-state Markov chain. However, in such situations the diffusion process will still remain within the interval $[0, 1]$ because of the reflecting boundary condition

(8). Therefore the probability of the process, $Y(t)$, described by (5) and (8) lying outside the interval $[0,1]$ is 0. Yet, as discussed in the last section, the solutions to the SDE that describes the individual paths of this process can leave this region with positive probability.

In order to impose the boundary condition (8) on the dynamics of the SDE (6), consider decomposing the diffusion process $Y(t)$ into the sum of two stochastic processes $Y(t) = X(t) + K(t)$. The dynamics of the first process, $X(t)$, is governed by (6), and so determines the behaviour of $Y(t)$ on the interior of the interval $(0,1)$. Thus we must have that $Y(0) = X(0)$ and in particular it follows that $Y(t) = X(t)$ on $(0,1)$.

The process $K(t)$ determines the behaviour at the boundary and we set it to have initial value $K(t) = 0$. In some sense $K(t)$ can be thought of as the minimal process which forces $Y(t)$ to remain in the interval $[0,1]$. The measure induced by this process must thus be concentrated at the times t_e where $Y(t_e) = 1$ or $Y(t_e) = 0$. We can formalise this by requiring $K(t)$ to satisfy the following property,

$$|K|(t) = \int_0^t \mathbf{1}_{\{Y(s)=0, Y(s)=1\}} d|K|(s). \qquad (9)$$

In fact, in [44] the authors informally refer to the process $K(t)$ as a *local time*. In stochastic analysis the *local time* is a process that characterises the amount of time a stochastic process spends at a particular point. So by using this term, the authors in [44] are emphasising that the measure of $K(t)$ is closely linked to the amount of time $Y(t)$ spends at the boundary.

The property above only ensures that $K(t)$ changes at the times when $Y(t)$ is at the boundary, but the way in which $K(t)$ will reflect the process $Y(t)$ back into $(0,1)$ at the endpoints of this interval must still be specified. We assume that the process $K(t)$ will reflect $Y(t)$ into the interior of the interval in the direction of the inward pointing unit normal. That is, when $Y(t) = 0$, $K(t)$ will push the process in the positive direction while at $Y(t) = 1$, $K(t)$ will force this process in the opposite direction. To characterise the behaviour of $Y(t)$ at the boundary in this way we impose the following condition on $K(t)$

$$K(t) = \int_0^t \gamma(Y(s)) d|K|(s), \qquad (10)$$

where $\gamma(Y(s))$ is a unit inward normal to the endpoints of the interval $[0,1]$ and $|K|(t)$ denotes the total variation of $K(t)$ on $[0,t]$. Other authors also deal with oblique reflection at the boundary [45], however for our problem we focus only on normal reflection at the boundary.

Taking the stochastic differential it follows that $Y(t)$ satisfies the SDE

$$dY = (a - \alpha Y)dt + \tfrac{1}{\sqrt{N}}\sqrt{a + \beta Y}\, dW + dK, \quad (11)$$

with initial condition $Y(0) = y_0 \in [0,1]$. Such an equation is termed a reflected SDE, since the process $Y(t)$ is instantaneously reflected back into $[0,1]$ when it reaches the endpoints. We shall refer to the domain into which the reflected SDE forces the solution as the reflecting domain. This equation is also sometimes known as the Skorokhod equation, since Skorokhod first proved the existence and uniqueness of solutions to SDEs of this type [46], [47].

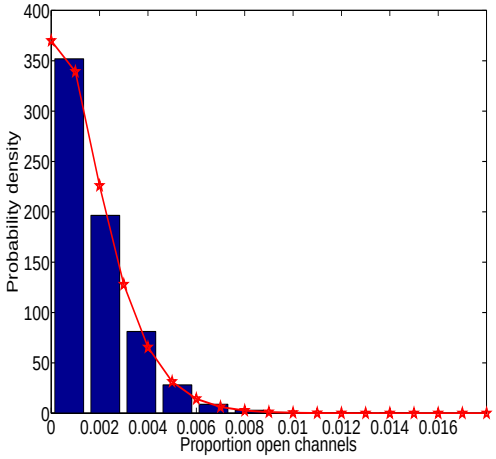

FIG. 1: (Color online) A frequency plot of the reflected SDE for the simple 2 state model calculated over $100,000$ simulations with parameter values $N = 500$, $a = 0.004$, $b = 3$ and the initial proportion of open channels set to 0.1 (blue (dark gray) bars). Solution of the Fokker-Planck equation for the same parameter values (red (light gray) line with star markers). Both distributions are calculated after $4ms$ of simulation.

To better understand this reflecting process $K(t)$, we shall for a moment digress from our current domain of reflection, and consider the simplest situation where the process $Y(t)$ is reflected at 0 (i.e. the domain of reflection is $[0,\infty)$). The smallest value that would have to be added to the process to ensure that it remains in $[0,\infty)$ in the time interval $[0,t]$, will be the maximum amount by which the unreflected process overshoots the zero boundary (i.e. the largest negative value of the unreflected

process) up until time t. That is, the exact form of the reflecting process in this simple case will be

$$K(t) = sup_{0\leq s\leq t}(Y(s))^{-}, \quad \text{where } a^{-} = max(0,-a). \tag{12}$$

In our case there is also reflection at the boundary $y = 1$ and so $K(t)$ will no longer take the form given above. In general it is difficult to characterise the reflecting process $K(t)$ for an arbitrary reflecting domain and so it must be approximated numerically. In Sec. V we shall discuss numerical methods to approximate solutions to reflected SDEs.

In Fig. 1 we compare the probability distribution obtained from solving (5) with boundary conditions (8) with the distribution obtained from multiple simulations of the reflected SDE (11). The two distributions are very similar, supporting the conclusion that the reflected SDE is the correct formulation of the sample paths for the process described by (5) and (8).

IV. GENERALISATION TO MULTISTATE ION CHANNEL MODELS

The model of ion channel dynamics considered so far is somewhat an over-simplification of true ion channel behaviour within cardiac and neuronal cells. More commonly a channel will reside in a number of different conformational states as it transitions to the open position and so more realistic models are far more complex than the two state model considered thus far (see [48], for example). We therefore discuss the extension of the reflected SDE framework to a multistate model of ion channel dynamics, where a channel can reside in one of m different states at time t.

As before, the total number of channels, N, is assumed to remain constant and the state of the system is now given by the vector $\boldsymbol{Y}(t) = (Y_1(t),\ldots,Y_m(t))^T$, whose entries $Y_i(t)$ are the proportion of channels in state i at time t. A channel can transition from one state to another via k different reversible transitions, so the total number of transitions possible in the system is $2k$. If transition l results in a channel in state i moving to state j then the probability of transition l occurring is $f_l(\boldsymbol{y}(t)) = r_{ij}y_i(t)$, where r_{ij} is the transition rate of the channel shifting from state i to j.

As for the simple model, the individual trajectories of the approximate continuous-state process can be described by the following Langevin SDE, [29], [26],

$$d\boldsymbol{Y} = A(\boldsymbol{Y})dt + \tfrac{1}{\sqrt{N}}\sqrt{B(\boldsymbol{Y})}d\boldsymbol{W}, \tag{13}$$

where $d\boldsymbol{W}$ is a vector of independent Wiener increments (for the specific forms of the matrices $A(\boldsymbol{Y})$ and $B(\boldsymbol{Y})$ see [26] and [29]).

This equation was first described by Fox and Lu [26] for the sodium and potassium channels in the Hodgkin-Huxley model and was later implemented by Goldwyn et al. [29]. The issue with (13) is that it involves the square root of a matrix, limiting the computational speed up over the discrete-state Markov chain model [29]. Therefore in [26] Fox and Lu describe a simplification by directly extending the Hodgkin-Huxley model, describing each gating variable by an SDE and this method has since been taken as the standard way to model ion channel dynamics using SDEs. This formulation, termed the subunit-based SDE in [29], provides substantial computational speed up over (13), but is inconsistent with the discrete-state Markov chain model [23], [27], [28], while the SDE model given by (13) is not [29], [30].

Due to the special structure of this system, namely that each transition is reversible, it is possible to decompose the matrix $B(\boldsymbol{Y})$ so that the square root can be described exactly by the product of two matrices, [49]. The decomposition of the matrix $B(\boldsymbol{Y})$ is non-unique, that is there are different matrices $\tilde{B}(\boldsymbol{Y})$ such that $\tilde{B}(\boldsymbol{Y})\tilde{B}(\boldsymbol{Y})^T = B(\boldsymbol{Y})$. In [49] the authors showed that the smallest dimension of the matrix $\tilde{B}(\boldsymbol{Y})$ that satisfies $\tilde{B}(\boldsymbol{Y})\tilde{B}(\boldsymbol{Y})^T = B(\boldsymbol{Y})$ is $m \times k$, and this matrix takes the form $\tilde{B}(\boldsymbol{Y}) = EF(\boldsymbol{Y})$. Here E is a matrix of $0's$, $-1's$, and $1's$ and $F(\boldsymbol{Y})$ is a diagonal matrix whose entries are of the form $\sqrt{r_{ij}y_i + r_{ji}y_j}$. Therefore (13) becomes [49]

$$d\boldsymbol{Y} = A(\boldsymbol{Y})dt + \tfrac{1}{\sqrt{N}}EF(\boldsymbol{Y})d\boldsymbol{W}. \tag{14}$$

For an example of the matrices E and $F(\boldsymbol{Y})$ for the sodium and potassium channels in the Hodgkin-Huxley model, see Appendix A. We use this formulation of the decomposition of the matrix B since it employs fewer Wiener increments than that given in [39] and so is more computationally efficient.

This formulation of the noise term will require a larger number of Wiener increments than the approach in [29], given by (13), when the number of reversible transitions is greater than the number of different states of the channel. For example, in the Hodgkin-Huxley model, the sodium channel is assumed to consist of 8 different states which can undergo 10 different pairs of reversible reactions. The

formulation of the SDE, (13), will require 8 Wiener increments at each time step while (14) will require 10 in this case. However, since all Wiener increments for the simulation can be initialised at the start, the extra computational cost in generating more Wiener increments per simulation is very minimal. Indeed, it is certainly much less computationally intensive than taking the square root of a matrix at each time step, and thus provides substantial improvement in speed over the implementation in [29].

For $\boldsymbol{Y}(t)$ to have biological meaning, each element, $Y_i(t)$ for $i = 1, \ldots, m$, of the vector must lie within the interval $[0, 1]$ since it represents the proportion of channels in state i at time t. Therefore it follows that the individual trajectories of this process, given by (13), must remain within a m-dimensional hypercube bounded by the intervals $[0, 1]$. Furthermore, by conservation of the number of channels, $\sum_{i=1}^{m} Y_i(t) = 1$, $\boldsymbol{Y}(t)$ is restricted to the hyperplane given by $\sum_{i=1}^{m} Y_i = 1$ which lies inside this hypercube. We denote the reflected domain of the process $\boldsymbol{Y}(t)$ by D. For a channel that can reside in three different states, for example, D will take the form of a plane, which is embedded within a cube, see Fig. 2.

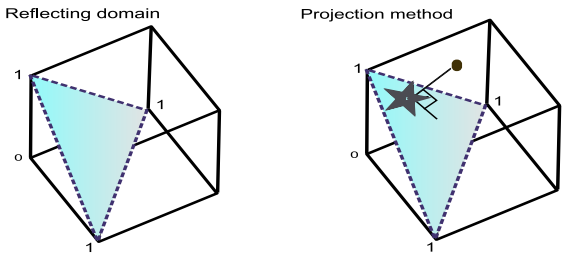

FIG. 2: (Color online) Left: Example of the reflecting domain, D, (shaded region) for an ion channel model that can reside in three different states. Right: Diagramatical representation of the projection scheme for an ion channel that can reside in three different states.

To ensure solutions to (13) remain within D, as in the previous section we decompose the process $\boldsymbol{Y}(t)$ into the sum of two processes $\boldsymbol{Y}(t) = \boldsymbol{X}(t) + \boldsymbol{K}(t)$. The first, $\boldsymbol{X}(t)$, satisfies (13), and describes the behaviour of $\boldsymbol{Y}(t)$ on the interior of the domain D ($int(D)$), i.e. $\boldsymbol{Y}(t) = \boldsymbol{X}(t)$ for $\boldsymbol{X}(t) \in int(D)$. The second, $\boldsymbol{K}(t)$, we again define to be the process that reflects $\boldsymbol{Y}(t)$ into D. As before we can describe the individual realisations of the process by a reflected SDE

$$d\boldsymbol{Y} = A(\boldsymbol{Y})dt + \tfrac{1}{\sqrt{N}} EF(\boldsymbol{Y})d\boldsymbol{W} + d\boldsymbol{K}. \qquad (15)$$

Analogously to the simple 2 state model, we can think of the reflecting process $\boldsymbol{K}(t)$, now vector-valued, as the minimal amount that we need to add to the unreflected process to ensure that $\boldsymbol{Y}(t)$ remains within the domain D. The definition of the conditions imposed on the reflecting process in the 2 state model, (9) and (10), naturally generalise to the multidimensional setting,

$$|\boldsymbol{K}|(t) = \int_0^t \mathbf{1}_{\{\boldsymbol{Y}(s)\in\partial D\}} d|\boldsymbol{K}|(s),$$

$$\boldsymbol{K}(t) = \int_0^t \gamma(s) d|\boldsymbol{K}|(s), \qquad (16)$$

where $\gamma(s) \in N(\boldsymbol{Y}(s))$ if $\boldsymbol{Y}(s) \in \partial D$ and $N(\boldsymbol{x})$ is the set of inward pointing unit vectors to the point $\boldsymbol{x}$ which lies on the boundary of D (∂D). The solution to the reflected SDE, (15) will be a pair $(\boldsymbol{Y}(t), \boldsymbol{K}(t))$ that satisfy these properties. For a more rigorous definition of the solution to the reflected SDE (15), see for example [50].

The existence and uniqueness of such a pair was extended to domains in $\mathbb{R}^n$ by [51], providing D is convex [52] or satisfies certain regularity conditions [53]. Since our domain D is convex, the solution to the reflected SDE that describes the behaviour of a general ion channel model, (15), exists and is unique. As for the simple model, the last two conditions in the above definition ensure that the reflecting process only increases on the boundary of D, ∂D, and that it reflects $\boldsymbol{Y}(t)$ back into the interior of D in the normal direction to the boundary.

Although numerical methods for reflected SDEs is a far less developed field than for ordinary SDEs, a number of techniques exist. These can be broadly split into two categories, penalization methods and projection methods. The penalization method constructs solutions to reflected SDEs by approximating diffusion processes where the reflecting process is replaced by a penalty term, $\beta_\lambda(y)$. Convergence to the solution of the reflected SDE is acquired in the limit as $\lambda \downarrow 0$. Such methods have been studied by [54], [55], [56] with orders of strong and weak convergence obtained under different conditions. The issue with such methods is that numerical solutions can leave the domain D, even though the exact solution to the reflected SDE does not. For this reason we do not use such methods. The projection method approximates the solution to the SDE without reflection, and if the numerical solution leaves D it is projected onto the domain. Such methods ensure numerical solutions remain within the desired

region. In the next section we describe an algorithm to obtain numerical solutions to the reflected SDEs given in this section using the projection method.

V. PROJECTION METHOD FOR REFLECTED STOCHASTIC DIFFERENTIAL EQUATIONS

The projection method is a simple extension of the Euler-Maruyama method, given in Sec. II. At time t the non-reflected process is evaluated at the next time step $t+\Delta_t$ using the Euler-Maruyama algorithm, (7). If this value lies within the closure of D, $\overline{D}$, then the process at the next time step is set to this value. Otherwise it is equal to the orthogonal projection of this point onto the boundary of D. Let $\Pi(\cdot)$ denote the orthogonal projection map onto D, given in the following subsection. For fixed time step, Δ_t, the projection method algorithm is as follows:

1. Set $t=0$ and $\boldsymbol{Y}(0)=\boldsymbol{y}_0$.
2. Generate ΔW_p, $p=1,\cdots,k$ as independent normal random variables mean 0 and variance Δ_t. Let $\Delta\boldsymbol{W}=[W_1,\ldots,W_k]^T$ and set
$$\boldsymbol{Y}_G(t+\Delta_t)=\boldsymbol{Y}(t)+A(\boldsymbol{Y}(t))\Delta_t + \tfrac{1}{\sqrt{N}}EF(\boldsymbol{Y}(t))\Delta\boldsymbol{W}. \quad (17)$$
3. If $\boldsymbol{Y}_G(t+\Delta_t)\in\overline{D}$ then set $\boldsymbol{Y}(t+\Delta_t)=\boldsymbol{Y}_G(t+\Delta_t)$. Otherwise $\boldsymbol{Y}(t+\Delta_t)=\Pi\left(\boldsymbol{Y}_{G(t+\Delta_t)}\right)$.
4. Set $t=t+\Delta_t$ and return to step two.

Fig. 2 diagrammatically shows how the projection method works at a certain time step for a three state model. The shaded area is the domain of reflection, the round point is the value at some time step of the unreflected process and the star point is the projection of this point onto D, i.e. the value taken at the next time step for the projection method.

Note that under this scheme we do not explicitly calculate the reflecting process $\boldsymbol{K}(t)$ at each time step since we are only interested in the solution to the reflected SDE, $\boldsymbol{Y}(t)$. However, it is straightforward to define $\boldsymbol{K}(t)$ for the numerical algorithm given above, $\boldsymbol{K}(0)=0$,

$$\boldsymbol{K}(t+\Delta_t)=\begin{cases}\boldsymbol{K}(t)+\Pi(\boldsymbol{Y}_G) & \text{if } \boldsymbol{Y}_G\notin\bar{D}\\ \boldsymbol{K}(t) & \text{otherwise.}\end{cases}$$

This scheme has been shown to converge in the mean square sense with order $O(\Delta_t^{1/2-\epsilon})$, for any $\epsilon>0$, uniformly on compact sets, [57]. In [50] a slightly faster rate of $O((\Delta_t log\Delta_t)^{1/2})$ was obtained but this was only for pointwise convergence. Therefore this scheme has a lower order of convergence than the standard Euler-Maruyama method. The lower convergence is due to the fact that between times t and $t+\Delta_t$ the process may leave $\overline{D}$ and lie in $\overline{D}$ at time $t+\Delta_t$ without any effect on the value of the numerical approximation at $t+\Delta_t$. This 'overshoot' of the approximation means that the projected method does not agree with the exact solution at the discrete time points, while for the standard Euler-Maruyama method it does. Therefore to improve the order of convergence, this issue with the overshoot must be dealt with. In [58] this is done by sampling from the exact distribution of the reflecting process at each time step, therefore restricting this method to systems where the reflecting process can be characterised exactly and this is not the case for our system.

A. The Orthogonal projection method

We briefly describe the orthogonal projection method that is used to numerically approximate solutions to (15), for more details see [59].

For any point $z\in\mathbb{R}^m$, the projection of z onto the closure of the domain D, $\bar{D}$, is the solution to the minimisation problem

$$u=arg\ min_{u\in\bar{D}}||u-z||, \quad (18)$$

and since D is closed and convex this set contains a unique point. Chen and Ye [59] show that using Moreau's identity [60], the solution to (18) can be simplified to a univariate minimisation problem. Furthermore they show that there are m possible choices for the solution to this problem that can be computed explicitly and u is the only one of these that falls within the correct interval. Below is an outline of the algorithm used for the orthogonal projection of a point $\boldsymbol{y}=(y_1,\ldots,y_m)^T\in\mathbb{R}^m$ onto the domain $D=\{\boldsymbol{x}\in\mathbb{R}^m: 0\le x_i\le 1, i=1,\ldots,m \text{ and } \sum_{i=1}^m x_i=1\}$. For more details see [59],

1. Sort $\boldsymbol{y}$ into ascending order and set $i=m-1$.
2. Compute $t_i=\frac{\sum_{j=i+1}^m y_j-1}{m-i}$. If $t_i\ge y_i$, set $\hat{t}=t_i$ and go to Step 4. Otherwise reduce i by 1 and redo Step 2 if $i\ge 1$ or go to Step 3 if $i=1$.
3. Set $\hat{t}=\frac{\sum_{j=1}^m y_j-1}{m}$.

4. Set the projection of $\boldsymbol{y}$ onto D to be $x = max((y - \hat{t}), 0)$.

VI. CONDUCTANCE MODEL WITH BOUNDED STOCHASTIC ION CHANNEL DYNAMICS

We consider the application of the reflected SDE method to the sodium and potassium ion channel dynamics in the original Hodgkin-Huxley model [16] as well as a variant of this model given in [27]. However, this method could be applied to any conductance model.

The Hodgkin-Huxley model, [16], describes the propagation of an AP (a rapid rise and fall in the cell membrane potential) through a squid giant axon. The cell membrane is modelled as a capacitor in parallel with three ionic currents, a potassium current I_K, a sodium current, I_{Na}, and a constant leakage current, I_L. Thus the membrane potential, V, is described by the following differential equation

$$\begin{aligned} C\frac{dV}{dt} =& - G_{Na}p_O^{Na}(V - E_N) - G_K p_O^K (V - E_K) \\ & - G_L(V - E_L) + I, \end{aligned} \tag{19}$$

where C is the membrane capacitance, I is the stimulus current, E_i is the reversal potential for the current of type i and G_L is the conductance of the leakage current. The conductance through the sodium and potassium channels is given by the product $G_i p_O^i$, for $i = Na$ and K, where G_i is the maximal conductance per ion channel of type i and p_O^i is the proportion of open channels of type i.

To compute the evolution in p_O^i, the classical Hodgkin-Huxley model assumes that each sodium channel consists of three identical activation gates, m, and one inactivation gate, h, while the potassium channel has four identical gates, n. Each gate, z, can be either open or closed at time t and transitions from closed to open and vice versa at rates $a_z(V)$, $b_z(V)$, respectively, that depend on the membrane potential V.

Under the assumption of large channel numbers, so that ion channel fluctuations can be ignored (as is the case in the original Hodgkin-Huxley model), the proportion of open channels is given by the product of the proportion of open gates, with the dynamics of each gating variable described by an ODE [16]. In the case when channel fluctuations are significant, the dynamics of each channel can be modelled as a discrete-state Markov chain. Letting each possible configuration of open and closed gates represent a different state of the channel, the Markov kinetics of the sodium and potassium channels are given by the following state diagrams respectively:

$$n_0 \underset{b_n}{\overset{4a_n}{\rightleftarrows}} n_1 \underset{2b_n}{\overset{3a_n}{\rightleftarrows}} n_2 \underset{3b_n}{\overset{2a_n}{\rightleftarrows}} n_3 \underset{4b_n}{\overset{a_n}{\rightleftarrows}} n_4$$

$$\begin{array}{ccccccc} m_0h_0 & \underset{b_m}{\overset{3a_m}{\rightleftarrows}} & m_1h_0 & \underset{2b_m}{\overset{2a_m}{\rightleftarrows}} & m_2h_0 & \underset{3b_m}{\overset{a_m}{\rightleftarrows}} & m_3h_0 \\ b_h\uparrow\downarrow a_h & & b_h\uparrow\downarrow a_h & & b_h\uparrow\downarrow a_h & & b_h\uparrow\downarrow a_h \\ m_0h_1 & \underset{b_m}{\overset{3a_m}{\rightleftarrows}} & m_1h_1 & \underset{2b_m}{\overset{2a_m}{\rightleftarrows}} & m_2h_1 & \underset{3b_m}{\overset{a_m}{\rightleftarrows}} & m_3h_1 \end{array}$$

Let $y_{ij}(t)$ denote the proportion of sodium channels with i open m gates and j open h gates at time t. Similarly let $x_i(t)$ denote the proportion of open potassium channels with i open n gates at time t. The channel is assumed to be in the open state only when all gating variables are open and so $p_O^{Na} = y_{31}(t)$ and $p_O^K = x_4(t)$, respectively. The state of the potassium channel at time t is given by the vector $\boldsymbol{x}(t) = (x_4, x_3, x_2, x_1, x_0)^T$ and the state of the sodium channel is denoted by $\boldsymbol{y}(t) = (y_{31}, y_{21}, y_{11}, y_{01}, y_{30}, y_{20}, y_{10}, y_{00})^T$. The SDE describing the dynamics of the sodium and potassium channels was first derived in [26] and later implemented in [29], [30]. We use the representation of the noise term in the SDE described in [49], which removes the need to find the square root of a matrix and so the sodium and potassium channel dynamics are given by the following SDEs, [32], [49]

$$d\boldsymbol{y} = H_{Na}\boldsymbol{y}dt + \tfrac{1}{\sqrt{N_{Na}}}E_{Na}F_{Na}(\boldsymbol{y})d\boldsymbol{W}^{Na}, \tag{20}$$

$$d\boldsymbol{x} = H_K\boldsymbol{x}dt + \tfrac{1}{\sqrt{N_K}}E_K F_K(\boldsymbol{x})d\boldsymbol{W}^K, \tag{21}$$

where F_{Na}, F_K, E_{Na}, E_K, H_{Na}, H_K are given in Appendix A. To ensure the stochastic dynamics of the sodium and potassium channels remain within a biologically realistic region, we incorporate the reflecting processes $\boldsymbol{K}^{Na}$ and $\boldsymbol{K}^K$ into (20) and (21), respectively, in the manner described in Sec. IV, giving

$$d\boldsymbol{y} = H_{Na}\boldsymbol{y}dt + \tfrac{1}{\sqrt{N_{Na}}}E_{Na}F_{Na}(\boldsymbol{y})d\boldsymbol{W}^{Na} + d\boldsymbol{K}^{Na}, \tag{22}$$

$$d\boldsymbol{x} = H_K\boldsymbol{x}dt + \tfrac{1}{\sqrt{N_K}}E_K F_K(\boldsymbol{x})d\boldsymbol{W}^K + d\boldsymbol{K}^K. \tag{23}$$

To the best of our knowledge, the formulation of the stochastic dynamics of the sodium and potassium channels in terms of reflected SDEs in the classical Hodgkin-Huxley model is novel.

VII. SIMULATIONS

We compare different statistics obtained from simulations of the Hodgkin-Huxley model using the reflected SDE formulation of ion channel dynamics, with those obtained from a discrete-state Markov chain model approach, under a range of simulation protocols. Individual trajectories of the discrete stochastic model are simulated using the stochastic simulation algorithm (SSA), [22]. This algorithm calculates the exponential waiting time τ until the next transition and updates the number of channels in each state based on the most likely transition to have occurred.

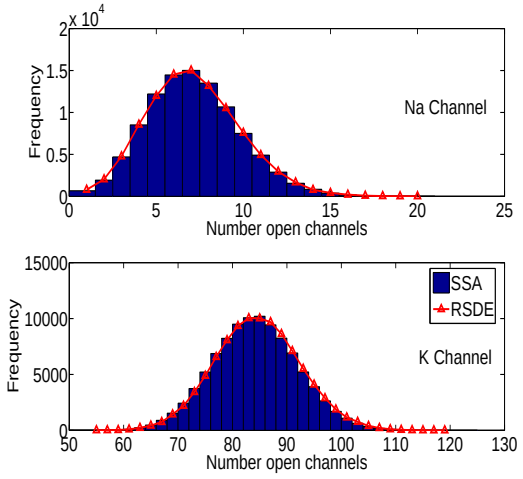

FIG. 3: (Color online) Distribution in the number of open sodium (top) and potassium (bottom) channels calculated using the reflected SDE (red (light gray) line with triangle markers) and the SSA (blue (dark gray) bars) where the number of sodium channels is set to 1000, the number of potassium channels is 333 and the voltage is set to $28mV$.

A. Open channel statistics

We calculated the mean and standard deviation in the proportion of open sodium and potassium channels in the Hodgkin-Huxley model, as given by (19). The total number of sodium and potassium channels was varied from 500 to 1000. For these simulations, the transition rates are taken to be the following functions of the membrane potential V [16],

$$a_m(V) = 0.1\frac{25-V}{e^{((25-V)/(10))}-1}, \quad b_m(V) = 4e^{\left(-\frac{V}{18}\right)},$$

$$a_h(V) = 0.07e^{\left(-\frac{V}{20}\right)}, \quad b_h(V) = \frac{1}{e^{((30-V)/(10))}+1},$$

$$a_n(V) = \frac{0.01\,(10-V)}{e^{((10-V)/10)}-1}, \quad b_n(V) = 0.125e^{\left(\frac{-V}{80}\right)}.$$

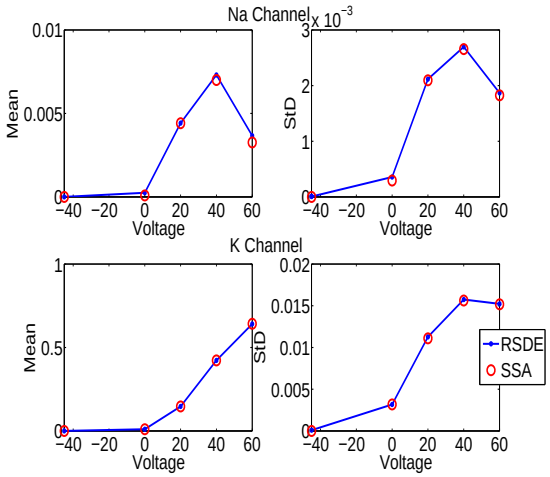

FIG. 4: (Color online) Mean (left) and standard deviation (right) in the proportion of open sodium (top) and potassium (bottom) channels calculated using the reflected SDE (blue (dark gray) line) and the SSA (red (light gray) circles). Statistics calculated over $100,000$ simulations at the final point for a fixed voltage value. In the reflected SDE simulations the initial condition for the sodium channel is taken to be $Y_0 = 1/8e^T$ and for the potassium channel it is $X_0 = 1/5e^T$, where e is the unit vector. For the discrete system the initial condition is calculated by multiplying Y_0 and X_0 by the number of sodium or potassium channels respectively, and rounding to the nearest whole number. The number of sodium and potassium channels is set to 1000 and the time step to $\Delta_t = 0.01ms$.

The mean and standard deviation were calculated over $100,000$ simulations and initially the voltage was kept constant throughout the simulation. Each simulation was run for a total of $100ms$, with the mean and standard deviation calculated at the final time point. The open channel statistics were calculated in this way for a range of different voltage values. Fig. 3 shows the distribution in the number of open sodium and potassium channels at the final simulation time point, where the voltage is set to $28mV$ (this value has been chosen arbitrarily). In Fig. 4 the mean and standard deviation in the number of open channels is plotted as a function of voltage, and the number of channels is set to 1000,

for the SSA and reflected SDE methods. The difference between the mean and standard deviation calculated using the two stochastic simulation methods (namely the SSA and reflected SDE) as a function of voltage for a range of difference channel numbers is shown in Fig. 5.

Next the open channel statistics were calculated for a fixed voltage path. Initially the deterministic Hodgkin-Huxley model was solved over $10ms$ with stimulus current $I = 10pA$ to obtain a path for the voltage that varies through time, shown in Fig 6. This path was then used to simulate the dynamics of the sodium and potassium channels over $10ms$ and the path statistics were calculated over $100,000$ simulations. Fig. 7 shows the mean and standard deviation in the number of open channels, as a function of time, where the number of channels is set to 1000, for the SSA and reflected SDE methods. The difference in the mean and standard deviation between these two stochastic simulation methods, is plotted as a function of time for a range of channel numbers in Fig. 8.

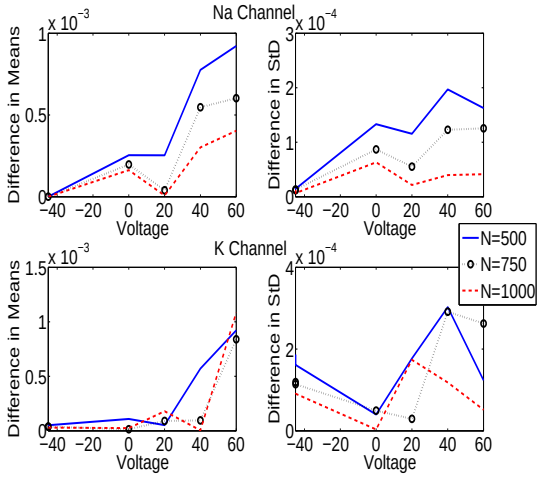

FIG. 5: (Color online) Absolute difference in the mean (left) and standard deviation (right) in the proportion of open sodium (top) and potassium (bottom) channels between the reflected SDE and the SSA for channel numbers equal to, $N = 500$ (blue (dark gray) solid line), $N = 750$, (black dotted line with circle markers) and $N = 1000$ (red (light gray) dashed line).

B. Action potential statistics

The comparison between the AP statistics calculated using the reflected SDE and the discrete-state Markov chain approach is an extension of simulations in [27]. In this study by Bruce, the effect of stochastic channel behaviour on the auditory fiber AP statistics were investigated as a function of the number of sodium channels (N_{Na}) using the metrics of the mean threshold current (I_{th}) and the relative spread (RS). The mean threshold current is the input current that corresponds to a firing efficiency (FE) of 50%, where FE is defined to be the fraction of trials in which the stimulus current results in the generation of an AP. It is calculated by fitting the FE versus input current curves using an integrated Gaussian function, as in [61]. The relative spread (RS) is a measure of the relative noise level and is calculated as,

$$RS = \frac{\sigma}{I_{th}}, \tag{24}$$

where σ is the standard deviation in threshold fluctuations and I_{th} is the threshold current. The jitter (standard deviation of AP occurrence times) and latency (mean value of AP occurrences) metrics were also used in the comparison of AP statistics between the reflected SDE and SSA simulation methods.

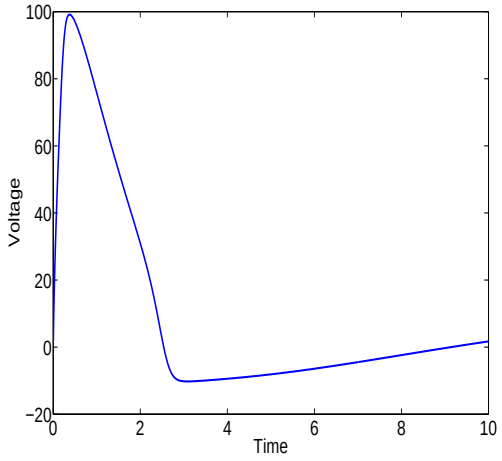

FIG. 6: (Color online) Voltage path used to calculate the open channel statistics for the sodium and potassium channels, for varying voltage simulations.

Since the examination of the AP statistics is based on the work of Bruce [27], we use the same equations as in this study in order to conduct these simulations, rather than using the classical Hodgkin-Huxley model as described in the previous subsection. For this model the membrane potential V is

described by the following equation

$$\frac{dV}{dt} = \frac{1}{C_m}\left(-\gamma_{Na} N_{Na}^{O}\left(V - E_{Na}\right) - \frac{V}{R_m} + I\right), \tag{25}$$

where C_m is the membrane capacitance, γ_{Na} is the single-channel sodium conductance, I is the stimulus current and N_{Na}^{O} is the number of open sodium channels. For the reflected SDE the value for N_{Na}^{O} is obtained by multiplying the proportion of open channels (from the SDE solution) by the total number of channels and rounding to the nearest integer. We employ this method of rounding since the work of Bruce [62] suggested that this is more accurate than either rounding up or down. Note that a potassium current has not been included in (25) mainly to ensure consistency with the simulations in [27] and so only the stochastic dynamics of the sodium channel are considered in the analysis of the AP statistics. The dynamics of the sodium channel are still modelled by the state diagram given in the previous section, however the transition rates are now taken to be the same functions of the voltage as were employed in the simulations in [27]

$$a_m = \frac{1.872(V - 25.41)}{1 - e^{(25.41-V)/6.06}}, \quad b_m = \frac{3.973(21.001 - V)}{1 - e^{(V+27.74)/9.41}},$$

$$a_h = \frac{-0.549(27.74 + V)}{1 - e^{(V+27.74)/9.06}}, \quad b_h = \frac{22.57}{1 - e^{(56-V)/12.5}}.$$

The AP statistics were calculated over 1000 repetitions of a single $100\mu s$ monophasic depolarising current pulse. The equation for the membrane potential, (25), is solved using the Euler method with a time step $\Delta_t = 1\mu s$. The stochastic dynamics of the sodium channel were simulated using the SSA and reflected SDE method, as in the previous section, and also using the method given in [29]. In [29], the authors use the SDE without reflection to describe the dynamics of the sodium channel, (20). To ensure solutions remain real the values y_{ij} in the noise term are replaced by their equilibrium values, and so this term is independent of the state of the system. When discussing the results we shall refer to this approach as the SDE method for simplicity. The threshold current I_{th} and the relative spread RS were calculated for sodium channel numbers ranging from 100 to 10,000. The effect of varying the total number of channels was considered for two different cases: constant channel density and constant membrane area. As described in [63], the membrane area is scaled proportionally to the number of channels in the case of constant channel density. Assuming the model's capacitance and resistance are based on 1000 sodium channels, as in [27], in the constant channel density simulations these values will be scaled by the total number of sodium channels N_{Na} (ranging from 100 to 10,000) as follows

$$C_m = 0.0714 \times \frac{N_{Na}}{1000} pF, \quad R_m = 1953.49 \times \frac{1000}{N_{Na}} M\Omega.$$

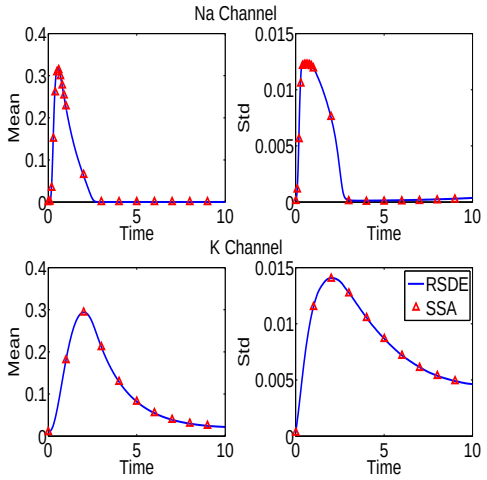

FIG. 7: (Color online) Mean (left) and standard deviation (right) in the proportion of open sodium (top) and potassium (bottom) channels calculated using the reflected SDE (blue (dark gray) line) and the SSA (red (light gray triangles)) for a set voltage path. The initial condition is the steady state for $V = 0$ of the deterministic system and the number of channels is set to be 1000.

For constant membrane area the capacitance and resistance are independent of N_{Na} and so are taken to be $C_m = 0.0714pF$ and $R_m = 1953.49M\Omega$ for all values of N_{Na}, as in [27]. These parameter values have been chosen primarily to ensure consistency with the simulations in the study by Bruce [27]. We remark that there is naturally variability in parameter values between cells, but we do not consider the effects of extrinsic noise in this paper and results are based solely on the values given here. The jitter and latency were calculated only for $N_{Na} = 1000$ channels. For more details of the simulation protocol used to calculate the AP statistics see [27] and the MATLAB code therein. In Fig. 9 the RS and threshold current, as calculated using the three different methods, are plotted as a function of the number of channels for the constant area and constant density scaling protocols. The top of Fig. 10 shows the difference in the RS between the SSA and reflected

SDE and the SSA and SDE method as a function of the number of channels, for constant density and constant area. The difference in the jitter and latency between the SSA and reflected SDE, and the SSA and SDE method, are shown at the bottom of Fig. 10 as a function of the stimulus current (I) and where the number of channels is set to 1000.

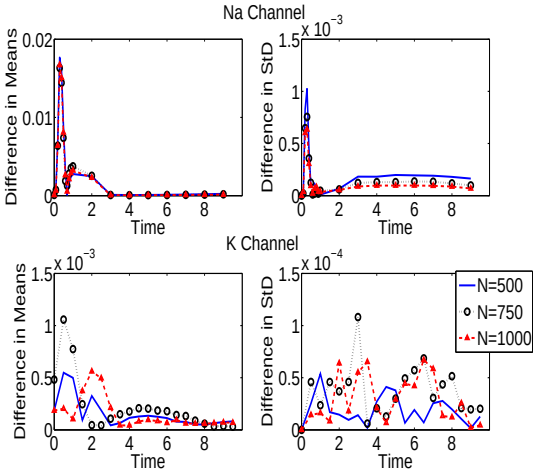

FIG. 8: (Color online) Absolute difference in the mean (left) and standard deviation (right) in the proportion of open sodium (top) and potassium (bottom) channels between the reflected SDE and the SSA for a fixed voltage path and channel numbers equal to, $N = 500$ (blue (dark gray) solid line), $N = 750$, (black dotted line with circle markers) and $N = 1000$ (red (light gray) dashed line with triangle markers).

Sample MATLAB code used for the simulations is available on the authors website and on the ModleDB website (accession number 144489).

VIII. RESULTS

A. Open channel statistics

When the voltage is kept fixed, the mean and standard deviation obtained using the reflected SDE is very close to that of the SSA for both the sodium and potassium channels, Fig. 4. In particular, the difference between the two means is on the order of 10^{-3} and as the number of channels increases it is clear that the reflected SDE mean converges to that of the SSA, as expected, Fig. 5. These quantitative results suggest that the reflected SDE accurately captures the distributional properties of the discrete-state Markov chain model. Furthermore, Fig. 3 qualitatively shows that the distribution in the number of open sodium and potassium channels for the reflected SDE is very similar to that of the discrete-state Markov chain. Therefore, when the voltage is kept constant these results suggest that the reflected SDE is an accurate approximation for the dynamics of the discrete-state Markov chain model.

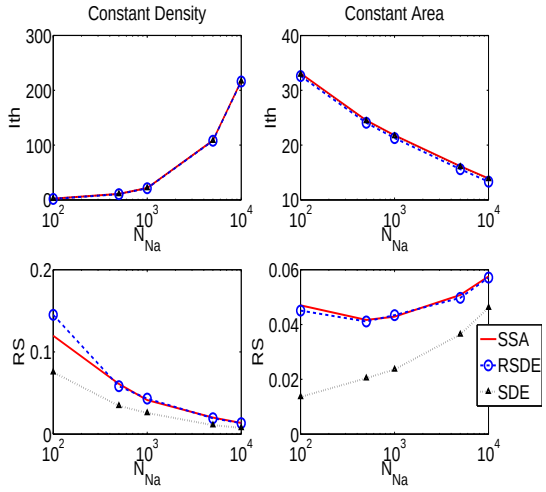

FIG. 9: (Color online) Threshold current (Ith) (top) and relative spread (RS) (bottom) as a function of the total number of sodium channels for constant channel density simulations (left) and constant membrane area simulations (right) calculated using the three different methods, SSA (red (light gray) solid line), reflected SDE method (blue (dark gray) dashed line with circle markers) and the SDE method from [29] (black dotted line with triangle markers).

For a set voltage path, the reflected SDE still closely matches the mean and standard deviation of the SSA simulations, Fig. 7. In particular, the difference in the means between the reflected SDE and SSA methods is on the order of 10^{-2} for the sodium channel and 10^{-3} for the potassium channel. The greatest difference between the two statistics occurs at the height of the AP, Fig. 8, and is likely to happen here since this is where the greatest voltage change (and so the greatest change in channel transition rates) between consecutive time steps takes place. In additional simulations (not shown), where the step-size was reduced, the greatest difference between the two statistics still occurred at the height of the AP, indicating that this effect is not a function of the time step. These results suggest that even with the added complication of a varying voltage in the ion channel model, the reflected SDE still accurately captures the open channel statistics

of the discrete-state Markov chain model.

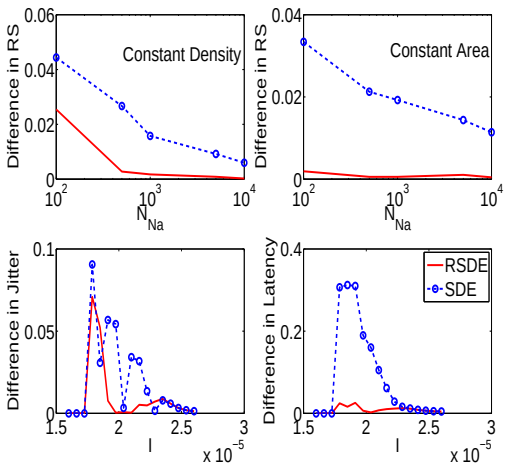

FIG. 10: (Color online) Top: Absolute differences in the relative spread (RS) between the SSA and reflected SDE methods (red (lower) line) and between the SSA and SDE methods (blue dashed (upper) line with circle markers). Results shown as a function of number of channels for constant channel density simulations (left) and constant membrane area simulations (right). Bottom: Absolute difference in the jitter (left) and latency (right) between the SSA and reflected SDE methods (red (dark gray) solid line) and between the SSA and SDE methods (blue (light gray) dashed line with circles). Results shown as a function of stimulus current for 1000 sodium channels.

B. Action potential statistics

From Fig. 9 it can be seen that the RS calculated from the reflected SDE simulations is very close to that of the SSA simulations and the two values quickly converge as the number of channels increases. This is the case for both the constant channel density and constant membrane area simulations. On the other hand, the difference between the RS for the SDE and the SSA simulations is noticeable even for large channel numbers, particularly in the case of the constant membrane area simulations, Fig. 10. Furthermore, the difference in the jitter and latency statistics between the reflected SDE and SSA simulations is much smaller than the difference between the SDE and SSA simulations, Fig. 10. These results suggest that the reflected SDE captures the AP statistics of the discrete-state Markov chain model more accurately than the SDE method in [29]. In the next section we shall discuss a possible reason for this.

Another advantage of the reflected SDE method is that simulations remain within a biologically realistic domain with probability 1, by definition. Without the reflecting term, however, with $100,000$ simulations of the Hodgkin-Huxley model given by (19), simulations went negative a mean number of 352 times.

Finally, Fig. 11 shows that the simulation time for the reflected SDE is substantially faster than the SSA, particularly for larger numbers of channels. In particular, the speed of the Markov chain model increases with increasing numbers of channels, while the reflected SDE method remains more or less constant. This is because the computational cost of the reflected SDE is dependent on the step-size used in simulation while the Markov chain model is restricted by the average time until the next reaction, which can become very small for large channel numbers.

Together, the results from the simulations suggest that the reflected SDE method is an accurate approximation of the discrete-state Markov chain model as well as ensuring biologically realistic and computationally efficient simulations.

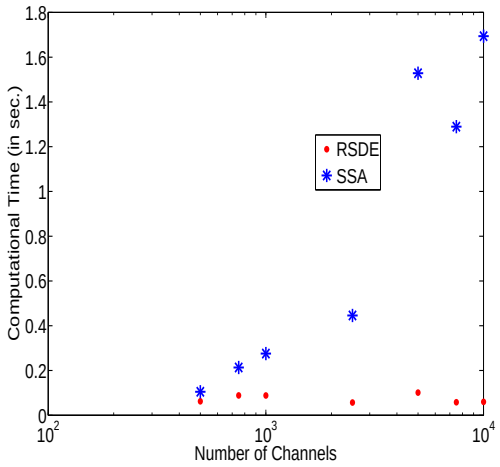

FIG. 11: (Color online) Mean computational time in seconds over $10,000$ simulations of the stochastic Hodgkin-Huxley model, (19), over $10ms$ for the reflected SDE approach (red (dark gray) dots) and the SSA approach (blue (light gray) stars) for a range of channel numbers. The time step in the reflected SDE simulations is taken to be $0.01ms$. Simulations were performed in MATLAB on a 2.5GHz core Intel Core 2 processor.

IX. DISCUSSION

SDEs were first introduced as a model of ion channel dynamics by Fox and Lu [26], who used them to describe the stochastic behaviour of the sodium and potassium channels in the Hodgkin-Huxley model. Since then, the approach taken by Fox and Lu has become the standard manner by which to model ion channel behaviour using SDEs within the neuroscience and cardiac modelling literature. The SDE model poses an attractive alternative to the discrete-state Markov chain approach for studying the effects of stochastic ion channel behaviour on the dynamics of electrically excitable cells and tissue due to the appreciable computational speed up achieved. For this reason they have been frequently utilised to simulate ion channel dynamics within a range of different electrically excitable cells including neuronal cells [24], [25], cardiac myocytes [5], and pancreatic beta cells [7]. However, the accuracy of the SDE approach has come into question in recent years for two main reasons. Firstly a number of studies have demonstrated that the SDE approach does not faithfully capture the stochastic behaviour of the discrete-state Markov chain model [23], [27], [28]. Secondly solutions to the SDE model can become negative and even imaginary, and so in such situations have no physical meaning [31]. The first of these issues was recently dealt with by Goldwyn et al. [29] who showed that by formulating the SDE model in terms of the multistate structure of the ion channel (termed the channel-based SDE), the SDE model accurately captures the stochastic behaviour of the discrete-state Markov chain model. However, they do not address the problem that the SDE can result in the proportion of channels in a certain state becoming negative. Indeed, the authors in [29] approximate the noise term by its equilibrium value so that simulations do not become imaginary, although they may still become negative.

In this paper we primarily address this issue that the SDE model can result in biologically unrealistic simulations of stochastic ion channel dynamics. We have demonstrated that by including a reflected term into the SDE, solutions are guaranteed to remain within a biologically realistic domain, whilst without this term they are not. We argued that this novel formulation is the correct equation that describes the individual realisations of the diffusion process, whose probability distribution is described by a Fokker-Planck equation obtained in the limit of large N from the Master equation that determines the discrete-state Markov chain. Thus we conclude that the reflected SDE provides a model of ion channel dynamics that is biologically realistic and mathematically consistent with the approximation from the discrete-state system to the continuous diffusion model. Furthermore, we have shown how to formulate the noise term in the SDE in terms of the product of two matrices, rather than as the square root of a matrix as was the approach in [29], thus greatly improving the computational efficiency over the implementation described in [29].

We present numerical results for the reflected SDE method applied to the classical Hodgkin-Huxley model for channel numbers ranging from 500 to 1000 both when the voltage is kept constant and when it was allowed to vary. From these simulations we show that the open channel statistics of the reflected SDE model are in good agreement with the discrete-state Markov chain model. Furthermore, the AP statistics for a variant of the Hodgkin-Huxley model given in [27] calculated using the reflected SDE were close to the discrete-state Markov chain model. In particular, the reflected SDE method seemed to perform better in these simulations than the approximate SDE method described in [29].

At channel numbers smaller than 500 the approximation to the reflected SDE begins to break down, and so it is possible that for such small channel numbers the behaviour of the reflected SDE will be less representative of the dynamics of the discrete-state Markov chain model. However, as can be seen in Fig. 11, at such channel numbers the computational cost of simulating the dynamics to the discrete-state Markov chain (namely using the SSA) is comparable to that of the reflected SDE. Therefore in such situations, the SSA would be the obvious simulation choice, since there is no gain to be made by using the approximate reflected SDE method.

A possible explanation for why the approach of Goldwyn et al. [29] does not perform as well as the reflected SDE here could be because the approximation made in the diffusion term, replacing the variables by their equilibrium value, may not be valid for the variant of the Hodgkin-Huxley model given by (25). The authors state in [29] that this approximation is accurate if "the relaxation of V to its equilibrium value occurred on a much slower time scale than the relaxation of the gating variables" and furthermore they note that "this separation of time scales does not appear to be a generic feature of Hodgkin-Huxley models". Therefore for this particular model, the approximation made in the diffusion term of the SDE may not be accurate enough to calculate the AP statistics studied here. However, in [29] the authors show that this approximation accu-

rately captures the mean open channel statistics as well as the mean and coefficient of variation of the interspike intervals in the classical Hodgkin-Huxley model. Therefore it seems that for certain models, the results from the approximate SDE method in [29] are comparable to the discrete-state Markov chain model, while for other models, namely those with fast AP dynamics, this method is less accurate than the reflected SDE. Finally we demonstrated that the reflected SDE approach is more computationally efficient than the discrete-state Markov chain simulation method, and for large numbers of channels the speed up can be an order of magnitude greater.

Since the field of numerical approximations to reflected SDEs is much less well developed than for ordinary SDEs, and since the work presented here was primarily concerned with modelling rather than numerical issues, the method used to solve the reflected SDE has a rather low order of convergence. A numerical scheme with a higher order of convergence may therefore result in better agreement between the reflected SDE and discrete-state Markov chain method. The development of such techniques is left to future work.

In this paper we have focused on stochastic models of ion channel dynamics. However, the issue of physically unrealistic solutions to the SDE model used to approximate discrete physical systems is present in a number of other fields, such as biochemical reaction kinetics [64]. The ideas presented in this paper could easily be extended to model such systems and so the method described here provides a general framework for modelling stochastic dynamics of physical systems by approximate methods in an accurate and efficient way.

We close by emphasising the combined contribution of this paper with the previous work of Goldwyn et al. [29] is to present an approximate formulation of the discrete-state Markov chain model for ion channel dynamics that gives significant computational speed up in simulation time, whilst preserving the stochastic behaviour and boundaries of the discrete-state system. This work therefore opens up the potential to accurately investigate the effects of stochastic ion channel behaviour in complex multiscale models, an area previously restricted by the computational cost of the discrete-state Markov chain approach.

ACKNOWLEDGMENTS

The author Ciara E. Dangerfield is funded by the EPSRC via the LSI doctoral training program.

Appendix A: Matrices Used in Numerical Simulations

$$F_{Na} = diag\begin{pmatrix} \sqrt{a_m y_{21}+3b_m y_{31}} \\ \sqrt{2a_m y_{11}+2b_m y_{22}} \\ \sqrt{3a_m y_{01}+b_m y_{11}} \\ \sqrt{a_m y_{20}+3b_m y_{30}} \\ \sqrt{2a_m y_{10}+2b_m y_{20}} \\ \sqrt{3a_m y_{00}+b_m y_{10}} \\ \sqrt{a_h y_{00}+b_h y_{01}} \\ \sqrt{a_h y_{10}+b_h y_{11}} \\ \sqrt{a_h y_{20}+b_h y_{21}} \\ \sqrt{a_h y_{30}+b_h y_{31}} \end{pmatrix} \qquad F_K = diag\begin{pmatrix} \sqrt{a_n x_3+4b_n x_4} \\ \sqrt{2a_n x_2+3b_n x_3} \\ \sqrt{3a_n x_1+2b_n x_2} \\ \sqrt{4a_n x_0+b_n x_1} \end{pmatrix},$$

respectively, and

$$H_{Na} = \begin{pmatrix} -(b_h+3b_m) & a_m & 0 & 0 & a_h & 0 & 0 & 0 \\ 3b_m & -(a_m+2b_m+b_h) & 2a_m & 0 & 0 & a_h & 0 & 0 \\ 0 & 2b_m & -(2a_m+b_m+b_h) & 3a_m & 0 & 0 & a_h & 0 \\ 0 & 0 & b_m & -(3a_m+b_h) & 0 & 0 & 0 & a_h \\ b_h & 0 & 0 & 0 & -(a_h+3b_m) & a_m & 0 & 0 \\ 0 & b_h & 0 & 0 & 3b_m & -(a_h+a_m+2b_m) & 2a_m & 0 \\ 0 & 0 & b_h & 0 & 0 & 2b_m & -(2a_m+b_m+a_h) & 3a_m \\ 0 & 0 & 0 & b_h & 0 & 0 & b_m & -(a_h+3a_m) \end{pmatrix}$$

$$E_{Na} = \begin{pmatrix} -1 & 0 & 0 & 0 & 0 & 0 & 0 & 0 & 0 & -1 \\ 1 & -1 & 0 & 0 & 0 & 0 & 0 & 0 & -1 & 0 \\ 0 & 1 & -1 & 0 & 0 & 0 & 0 & -1 & 0 & 0 \\ 0 & 0 & 1 & 0 & 0 & 0 & -1 & 0 & 0 & 0 \\ 0 & 0 & 0 & -1 & 0 & 0 & 0 & 0 & 0 & 1 \\ 0 & 0 & 0 & 1 & -1 & 0 & 0 & 0 & 1 & 0 \\ 0 & 0 & 0 & 0 & 1 & -1 & 0 & 1 & 0 & 0 \\ 0 & 0 & 0 & 0 & 0 & 1 & 1 & 0 & 0 & 0 \end{pmatrix}$$

$$H_K = \begin{pmatrix} -4b_n & a_n & 0 & 0 & 0 \\ 4b_n & -(a_n+3b_n) & 2a_n & 0 & 0 \\ 0 & 3b_n & -2(a_n+b_n) & 3a_n & 0 \\ 0 & 0 & 2b_n & -(3a_n+b_n) & 4a_n \\ 0 & 0 & 0 & b_n & -4a_n \end{pmatrix}$$

and

$$E_K = \begin{pmatrix} 1 & 0 & 0 & 0 \\ -1 & 1 & 0 & 0 \\ 0 & -1 & 1 & 0 \\ 0 & 0 & -1 & 1 \\ 0 & 0 & 0 & -1 \end{pmatrix}.$$

[1] F. Bezanilla, Physiol. Rev. **80**, 555 (2000).

[2] B. Hille, *Ionic Channels of Excitable Membranes* (Sinauer Associates, 1991), 3rd ed., ISBN 0878933239.

[3] B. Sakmann and E. Neher, *Single-channel Recording* (Plenum, New York, 1995).

[4] J. A. White, J. T. Rubinstein, and A. R. Kay, Trends in Neurosciences **23**, 131 (2000), ISSN 0166-2236.

[5] E. Pueyo, A. Corrias, L. Virág, N. Jost, T. Szél, A. Varró, N. Szentandrássy, P. P. Nánási, K. Burrage, and B. Rodríguez, Biophys Journal **12**, 2892 (2011).

[6] M. Lemay, E. de Lange, and J. P. Kucera, Journal of Theoretical Biology **281**, 84 (2011), ISSN 1095-8541.

[7] G. De Vries and A. Sherman, Journal of Theoretial Biology **207**, 513 (2000).

[8] J. R. Clay and L. J. DeFelice, Biophysical journal **42**, 151 (1983), ISSN 0006-3495, URL `http://dx.doi.org/10.1016/S0006-3495(83)84381-1`.

[9] E. Schneidman, B. Freedman, and I. Segev, Neural computation **10**, 1679 (1998), ISSN 0899-7667, URL `http://neco.mitpress.org/cgi/content/abstract/10/7/1679`.

[10] P. Oosterhoff, A. Oros, and M. A. Vos, Anadolu kardiyoloji dergisi : AKD = the Anatolian journal of cardiology **7 Suppl 1**, 73 (2007), ISSN 1302-8723, URL `http://view.ncbi.nlm.nih.gov/pubmed/17584687`.

[11] M. L. Martins, S. C. Ferreira, and M. J. Vilela, Current Opinion in Colloid & Interface Science **15**, 18 (2010), ISSN 13590294, URL `http://dx.doi.org/10.1016/j.cocis.2009.04.004`.

[12] J. R. Groff, H. DeRemigio, and G. D. Smith, *Markov chain models of ion channels and the collective gating of Ca2 + release sites* (Oxford: Oxford University Press, 2010), pp. 29–64.

[13] D. T. Gillespie, Physica A Statistical Mechanics and its Applications **188**, 404 (1992), ISSN 03784371.

[14] N. G. Van Kampen, *Stochastic Processes in Physics and Chemistry, Third Edition (North-Holland Personal Library)* (North Holland, 2007), 3rd ed., ISBN 0444529659.

[15] R. N. Bhattacharya and E. C. Waymire, *Stochastic Processes with Applications* (SIAM, 2009), 2nd ed.

[16] A. L. Hodgkin and A. F. Huxley, Journal of Physiology **117**, 500 (1952), ISSN 0092-8240.

[17] T. Austin, The Annals of Applied Probability **18**, 12791325 (2008).

[18] D. T. Gillespie, Annu. Rev. Phys. Chem. **58**, 35 (2007).

[19] T. Jahnke and W. Huisinga, Journal of Mathematical Biology **54**, 1 (2007), ISSN 0303-6812.

[20] S. MacNamara and K. Burrage, Numerical Algorithms **51**, 281 (2009), ISSN 1017-1398.

[21] C. Chow and J. White, Biophysical Journal **71**, 3013 (1996), ISSN 00063495.

[22] D. T. Gillespie, The Journal of Physical Chemistry **81**, 2340 (1977).

[23] H. Mino, J. T. Rubinstein, and J. A. White, Annals of Biomedical Engineering **30**, 578 (2002), ISSN 0090-6964.

[24] R. Fox, Biophysical Journal **72**, 2068 (1997), ISSN 00063495.

[25] X. J. Sun, J. Z. Lei, M. Perc, Q. S. Lu, and S. J. Lv, The European Physical Journal B - Condensed Matter and Complex Systems **79**, 61 (2011), ISSN 1434-6028, URL `http://dx.doi.org/10.1140/epjb/e2010-10031-3`.

[26] R. F. Fox and Y. N. Lu, Physical Review E **49**, 3421 (1994).

[27] I. C. Bruce, Annals of Biomedical Engineering **37**, 824 (2009), ISSN 1521-6047.

[28] B. Sengupta, S. B. Laughlin, and J. E. Niven, Physical review. E, Statistical, nonlinear, and soft matter physics **81** (2010), ISSN 1550-2376.

[29] J. H. Goldwyn, N. S. Imennov, M. Famulare, and E. Shea-Brown, Phys. Rev. E **83** (2011).

[30] J. H. Goldwyn and E. Shea-Brown, PLoS Comput Biol **7**, e1002247+ (2011), URL `http://dx.doi.org/10.1371/journal.pcbi.1002247`.

[31] C. E. Dangerfield, D. Kay, and K. Burrage, Procedia Computer Science **1**, 1581 (2010), ISSN 18770509.

[32] C. E. Dangerfield, D. Kay, S. MacNamara, and K. Burrage, BIT (2011).

[33] R. Lord, R. Koekkoek, and D. V. Dijk, Quantitative Finance **10**, 177 (2010).
[34] D. R. Brillinger, Lecture Notes-Monograph Series **41** (2003), ISSN 07492170.
[35] T. Kawamura and Y. Saisho, Stochastic Models **22**, 273 (2006), ISSN 1532-6349.
[36] D. Riley, X. Koutsoukos, and K. Riley, Simulation Conference, 2008. WSC 2008. Winter pp. 804–812 (2008).
[37] K. Pakdaman, M. Thieullen, and G. Wainrib, Adv. in Appl. Probab. **42**, 761 (2010).
[38] I. I. Gihman and A. V. Skorokhod, *Stochastic differential equations* (Berlin : Springer-Verlag, 1972).
[39] D. T. Gillespie, The Journal of Chemical Physics **113**, 297 (2000), ISSN 00219606.
[40] D. T. Gillespie, The Journal of Physical Chemistry A **106**, 5063 (2002).
[41] P. E. Kloeden and E. Platen, *Numerical Solution of Stochastic Differential Equations* (Springer, 2011), corrected ed., ISBN 9783540540625.
[42] J. C. Cox, J. E. Ingersoll, and S. A. Ross, Econometrica **53**, 385 (1985), ISSN 00129682.
[43] W. Feller, The Annals of Mathematics **54**, 173 (1951), ISSN 0003486X.
[44] C. Bayer, A. Szepessy, and R. Tempone, Monte Carlo Methods and Applications **16**, 1 (2010).
[45] M. Bossy, E. Gobet, and D. Talay, Journal of Applied Probability **41** (2004), ISSN 00219002.
[46] A. V. Skorokhod, Theory of Probability and its Applications **6**, 264 (1961).
[47] A. V. Skorokhod, Theory of Probability and its Applications **7**, 3 (1962).
[48] Y. Rudy and J. R. Silva, Quarterly reviews of biophysics **39**, 57 (2006), ISSN 0033-5835.
[49] B. Melykuti, K. Burrage, and K. C. Zygalakis, The Journal of Chemical Physics **132** (2010).
[50] R. Pettersson, Stochastic Processes and their Applications **59**, 295 (1995), ISSN 03044149.
[51] S. Wantanebe, J. Math. Kyoto Univ. **11**, 169 (1971).
[52] H. Tanaka, Hiroshima Math. J. **9**, 162 (1979).
[53] P. L. Lions and A. S. Sznitman, Communications on Pure and Applied Mathematics **37**, 511 (1984).
[54] Y. Liu, Mathematics and Computers in Simulation **38**, 103 (1995), ISSN 03784754.
[55] R. Pettersson, Bernoulli **3** (1997), ISSN 13507265.
[56] D. Ding, Computers & Mathematics with Applications **55**, 2413 (2008), ISSN 08981221.
[57] L. Slominski, Stochastic Processes and their Applications **50**, 197 (1994), ISSN 03044149.
[58] D. Lépingle, Mathematics and Computers in Simulation **38**, 119 (1995), ISSN 03784754.
[59] Y. Chen and X. Ye, arXiv:1101.6081 (2011), 1101.6081.
[60] P. L. Combettes and V. R. Wajs, Multiscale Modeling Simulation **4**, 1168+ (2005).
[61] A. A. Verveen and H. E. Derksen, Proceedings of the IEEE **56**, 906 (1968), ISSN 0018-9219.
[62] I. C. Bruce, Annals of Biomedical Engineering **35**, 315 (2007), ISSN 0090-6964, URL `http://dx.doi.org/10.1007/s10439-006-9174-9`.
[63] J. Rubinstein, Biophysical Journal **68**, 779 (1995), ISSN 00063495.
[64] D. Higham, IMA J Appl Math **76**, 449 (2011).